

Supporting Information

Water promoted 9-fluorenylmethyloxycarbonyl detachment from amino acid in charged microdroplets

Xiao-Fei Gao*, Jin-Cai Cheng, Chun-Lian Ye, Shan Xiao, Zai-Ming Qiu, Xinglei Zhang*

*Jiangxi Key Laboratory for Mass Spectrometry and Instrumentation, East China
University of Technology, Nanchang 330013, China*

Corresponding authors:

Dr. Xiao-Fei Gao, E-mail: sandy20025327@126.com, Prof. Xinglei Zhang,
leizi8586@126.com. Tel: (+86)791-8389-6370, Fax: (+86)791-8389-6370.

Table of Contents

Chemical and reagents.....	S3
Experimental setups.....	S3
Computational details	S4
Figure S1. Mass spectrometric analysis of Fmoc elimination reaction in microdroplets of P_f	S5
Figure S2. Mass spectrometric analysis of Fmoc elimination reaction in microdroplets of G_f with different distance	S6
Figure S3. Mass spectrometric analysis of Fmoc elimination reaction in microdroplets of P_f with different distance.....	S7
Figure S4. Mass spectrometric analysis of Fmoc elimination reaction in deuterated microdroplets of P_f	S8
Figure S5. Mass spectrometric analysis of Fmoc elimination reaction in microdroplets of A_f	S9
Figure S6. Mass spectrometric analysis of Fmoc elimination reaction in microdroplets of V_f	S10
Figure S7. Mass spectrometric analysis of Fmoc elimination reaction in microdroplets of L_f	S11
Figure S8. Mass spectrometric analysis of Fmoc elimination reaction in microdroplets of I_f	S12
Figure S9. Mass spectrometric analysis of Fmoc elimination reaction in microdroplets of M_f	S13
Figure S10. Mass spectrometric analysis of Fmoc elimination reaction in microdroplets of F_f	S14
Figure S11. Mass spectrometric analysis of Fmoc elimination reaction in microdroplets of K_f	S15
Figure S12. Mass spectrometric analysis of Fmoc elimination reaction in microdroplets of R_f	S16
Figure S13. Mass spectrometric analysis of Fmoc elimination reaction in microdroplets of GG_f	S17
Table S1 Relative proportion of [X _f - H] ⁻ and [X _c - H] ⁻ after microdroplet reaction recorded by mass spectrometer, comparing with base peaks in the mass spectra	S18
Cartesian coordinates, solution-phase Gibbs free energies and solution-phase enthalpies of intermediates and transition states	S20
References.....	S25

Chemicals and reagents

All chemical reagents were obtained from commercial suppliers and then directly used without further purification. Fmoc-Gly-OH (\geq 98%), Fmoc-Ala-OH (\geq 98%), Fmoc-Val-OH (\geq 98%), Fmoc-Leu-OH (\geq 98%), Fmoc-Ile-OH (\geq 98%), Fmoc-Pro-OH (\geq 98%), Fmoc-Met-OH (\geq 98%), Fmoc-Phe-OH (\geq 98%), Fmoc-Gly-Gly-OH (\geq 98%), Fmoc-Lys-OH (\geq 98%), Fmoc-Arg-OH (\geq 98%) and D₂O (99.9%) were purchased from Sun Chemical Technology (Shanghai) Co., LTD. HPLC grade methanol and acetonitrile solvent from Fisher Scientific (Nepean, ON, Canada) were used for all experiments. Deionized water was provided by the chemistry facilities in the East China Institute of Technology.

Experimental setup

All MS spectra were recorded in negative ion mode using a commercial linear ion trap mass spectrometer (LTQ-XL, ThermoFisher, San Jose, CA, USA). The mass spectrometer was coupled with a home-made n-ESI emitter (schematically shown in Figure 1a) for microdroplet generation and online analysis. The emitters were constructed from borosilicate glass capillaries (1.2 mm O.D., 0.9 mm I.D., World Precision Instruments Co.), that were pulled to a tip (~20 μ m, I.D.) using a Flaming/Brown micropipette puller (Sutter Instrument Co. model-1000, Novato, CA, U. S. A.). Xcalibur[®] software was used for LTQ instrument control and data processing.

The aqueous solution of the reactant without adding external catalysts or base was sprayed by the home-made n-ESI emitter, whose output was directed toward the

mass spectrometer inlet. All mass spectra were recorded for product analysis at -4.5 kV. Mass spectra were collected over an average time for 60 s in the *m/z* range of 50-500 at the centroid mode for each sample replicate. The temperature of the ion transfer capillary was 150 °C, the capillary voltage was -50.0 V, and the tube lens voltage was -150.0 V. Other parameters were default values recommended by the instrument manufacturer. Collision-induced dissociation (CID) experiments were performed on mass-selected ions for molecular structure identification using a collision energy (CE) in the range 0~30%, as indicated. The window width in MS/MS experiments for ions was 1.0 Da.

Computational Details

All calculations have been performed using the DFT method implemented in the commercial Gaussian 16^[1] program package. Molecular geometries of the model complexes were optimized applying the PBE0-D3BJ^[2-3]functional and Def2SVP^[4]basis set were used to describe all the atoms. As soon as the convergences of optimizations were obtained, the frequency calculations ate the same level have been performed to identify all the stationary points as minima or transition states, which has the unique imaginary frequencies. The intrinsic reaction coordinate (IRC)^[5] calculations have been carried out to confirm that the transition structures can indeed connect the related reactant and product. The optimized geometries mentioned were built by Gaussview 6.0^[6].

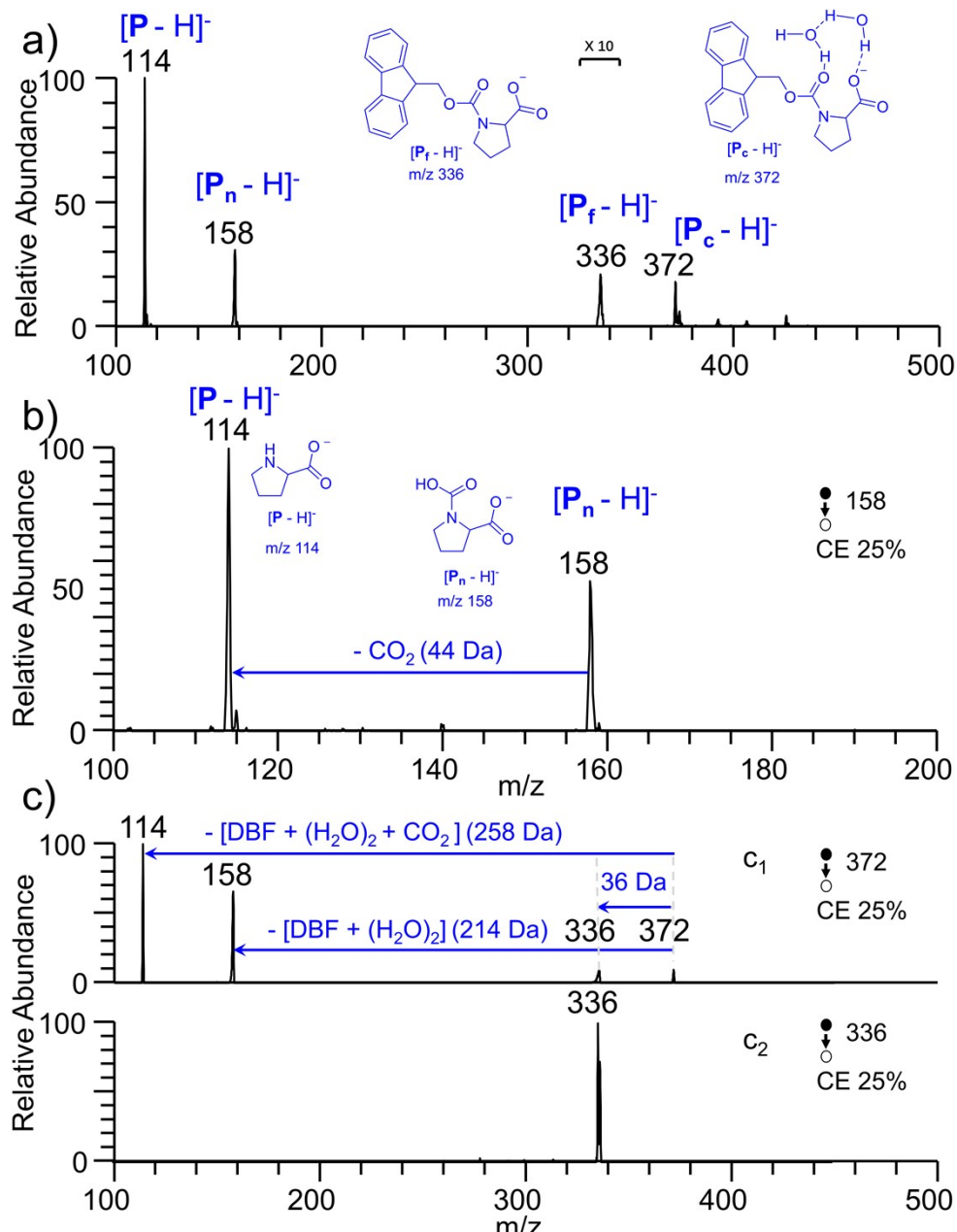


Figure S1. Mass spectrometric analysis of Fmoc elimination reaction in microdroplets of P_f. Online mass spectrum of Fmoc deprotection reaction of P_f in microdroplets (a). MS/MS spectra of ions of m/z 158 (b), m/z 372 (c₁), m/z 336 (c₂).

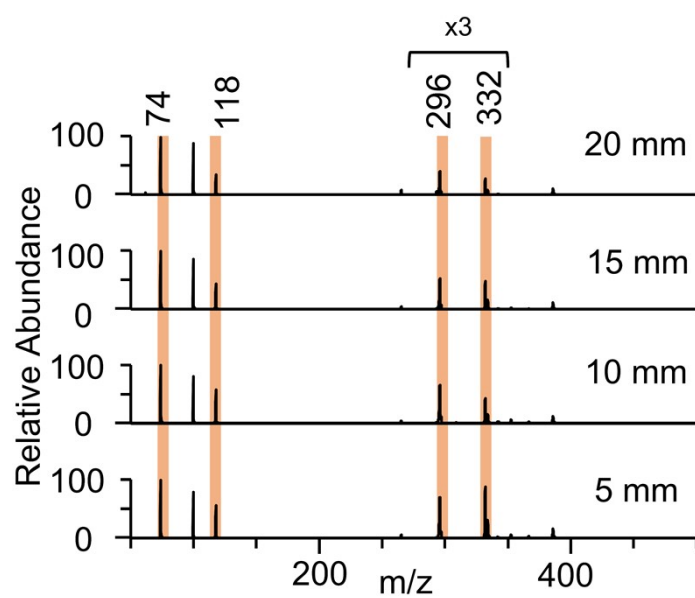


Figure S2 Mass spectrometric analysis of Fmoc elimination reaction in microdroplets of G_f with different distance.

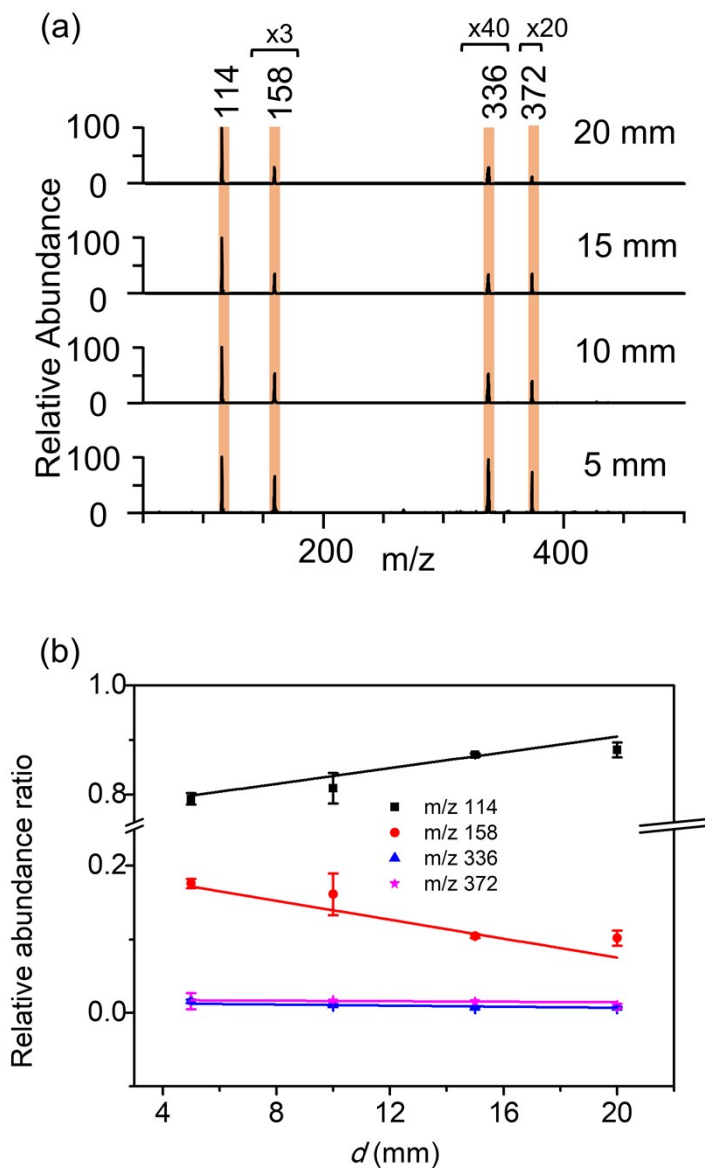


Figure S3 Fmoc elimination reaction in microdroplets of P_f with different distance. Online mass spectrum (a) and corresponding curves for relative abundance ratio of ions v.s. distance between tip of droplets emitter and inlet of droplets collector.

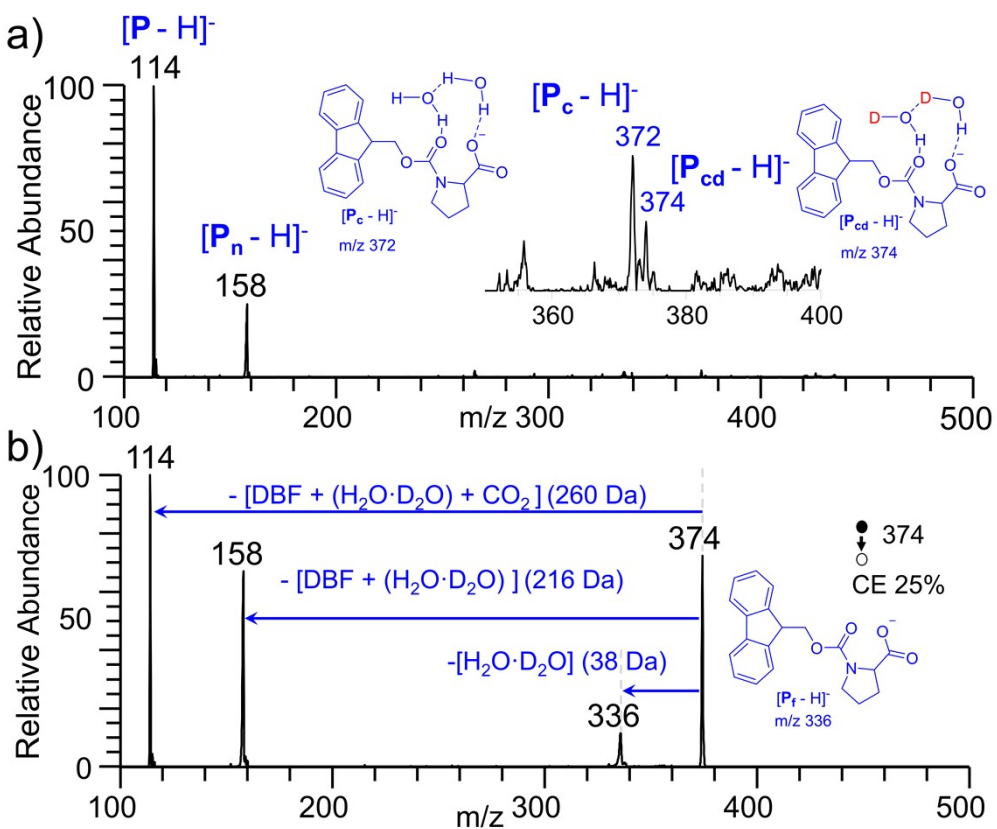


Figure S4. Mass spectrometric analysis of Fmoc elimination reaction in deuterated microdroplets of P_f . Online mass spectrum of Fmoc deprotection reaction of P_f in deuterated microdroplets (a). MS/MS spectra of ions of m/z 374.

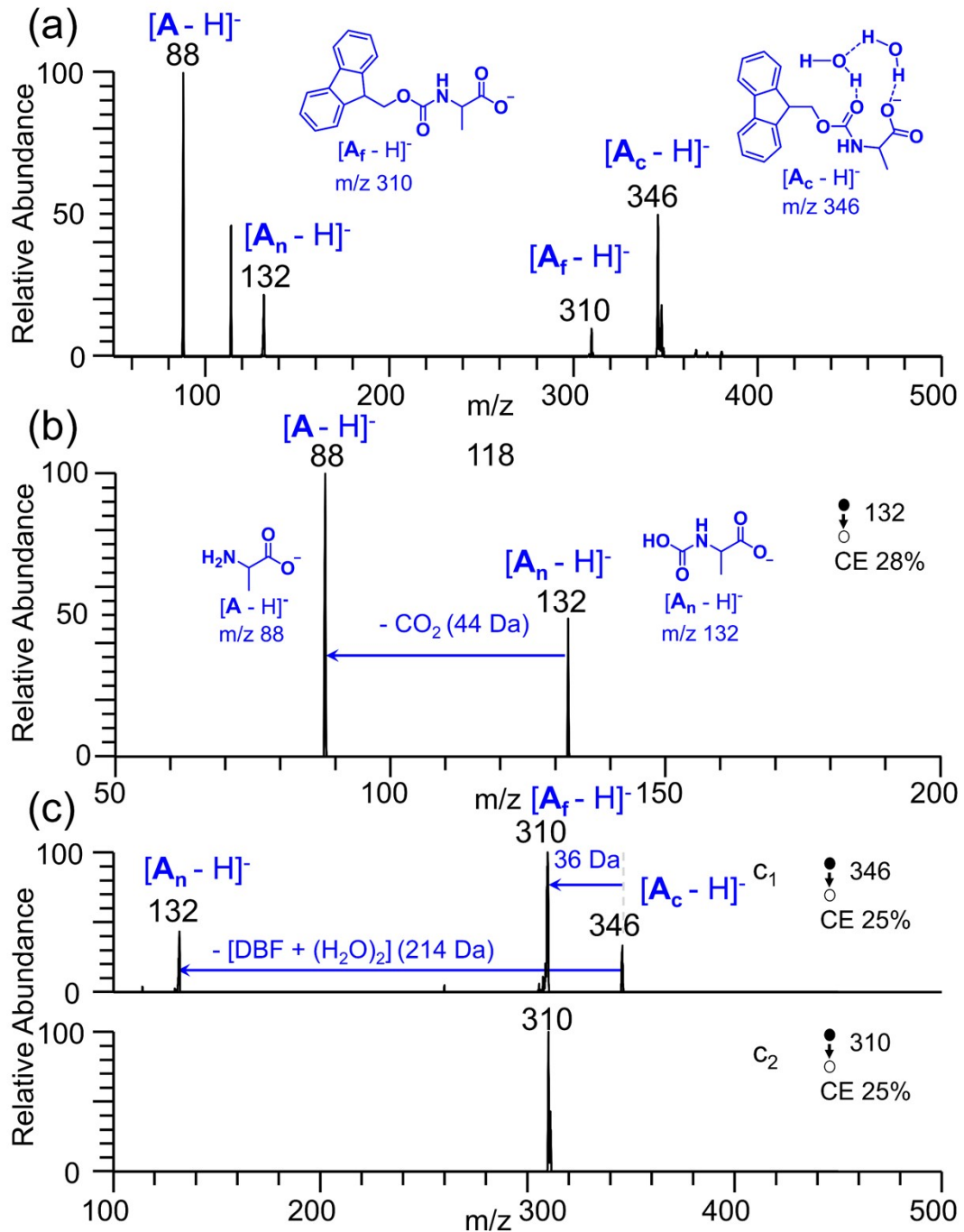


Figure S5. Mass spectrometric analysis of Fmoc deprotection reaction in microdroplets of \mathbf{A}_f . Online mass spectrum of Fmoc deprotection reaction of \mathbf{A}_f in microdroplets (a). MS/MS spectra of ions of m/z 132 (b), m/z 346 (c_1), m/z 310 (c_2).

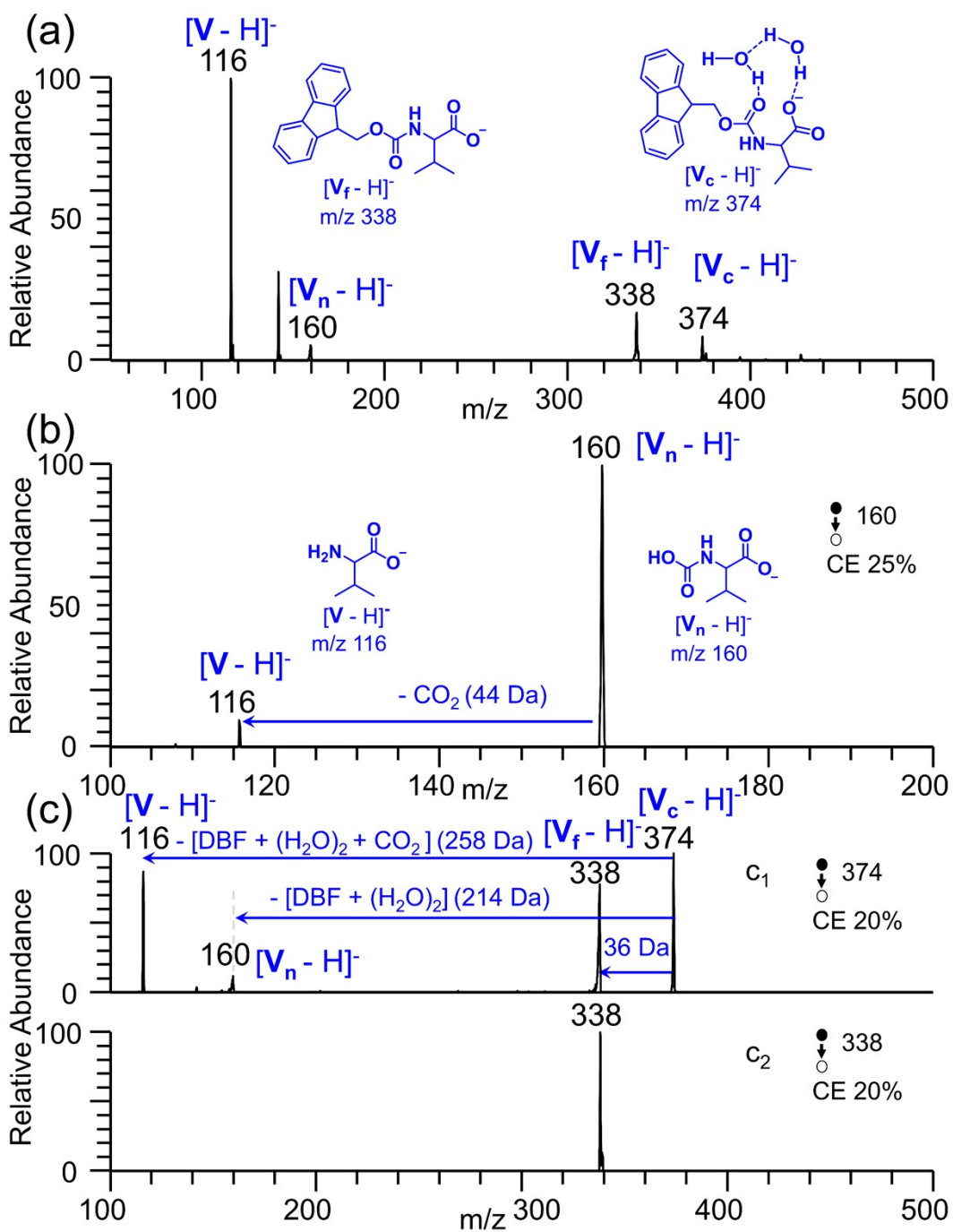


Figure S6. Mass spectrometric analysis of Fmoc elimination reaction in microdroplets of V_f . Online mass spectrum of Fmoc deprotection reaction of V_f in microdroplets (a). MS/MS spectra of ions of m/z 160 (b), m/z 374 (c_1), m/z 338 (c_2).

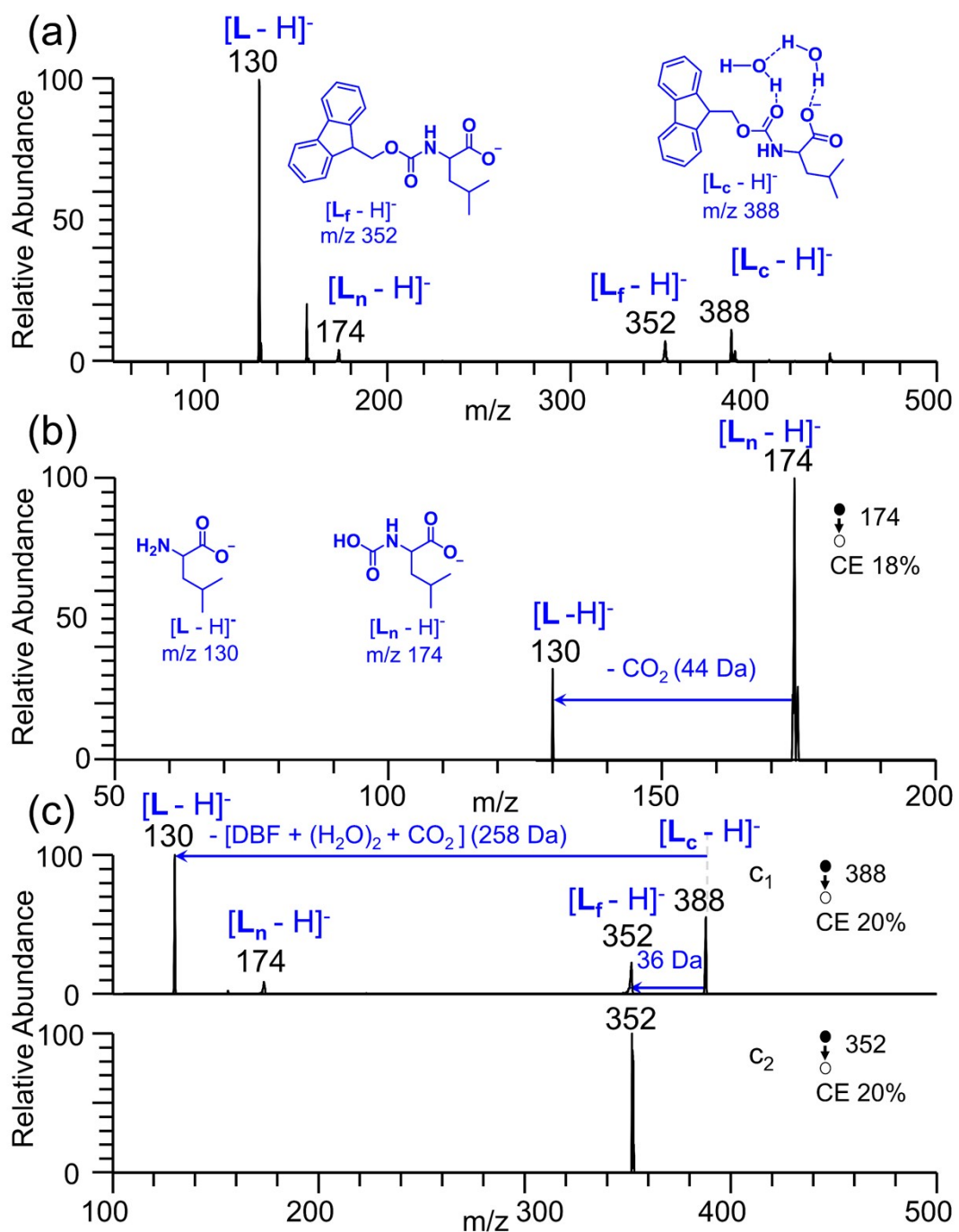


Figure S7. Mass spectrometric analysis of Fmoc elimination reaction in microdroplets of $\mathbf{L_f}$. (a) Online mass spectrum of Fmoc deprotection reaction of $\mathbf{L_f}$ in microdroplets. MS/MS spectra of ions of m/z 174 (b), m/z 388 (\mathbf{c}_1), m/z 352 (\mathbf{c}_2).

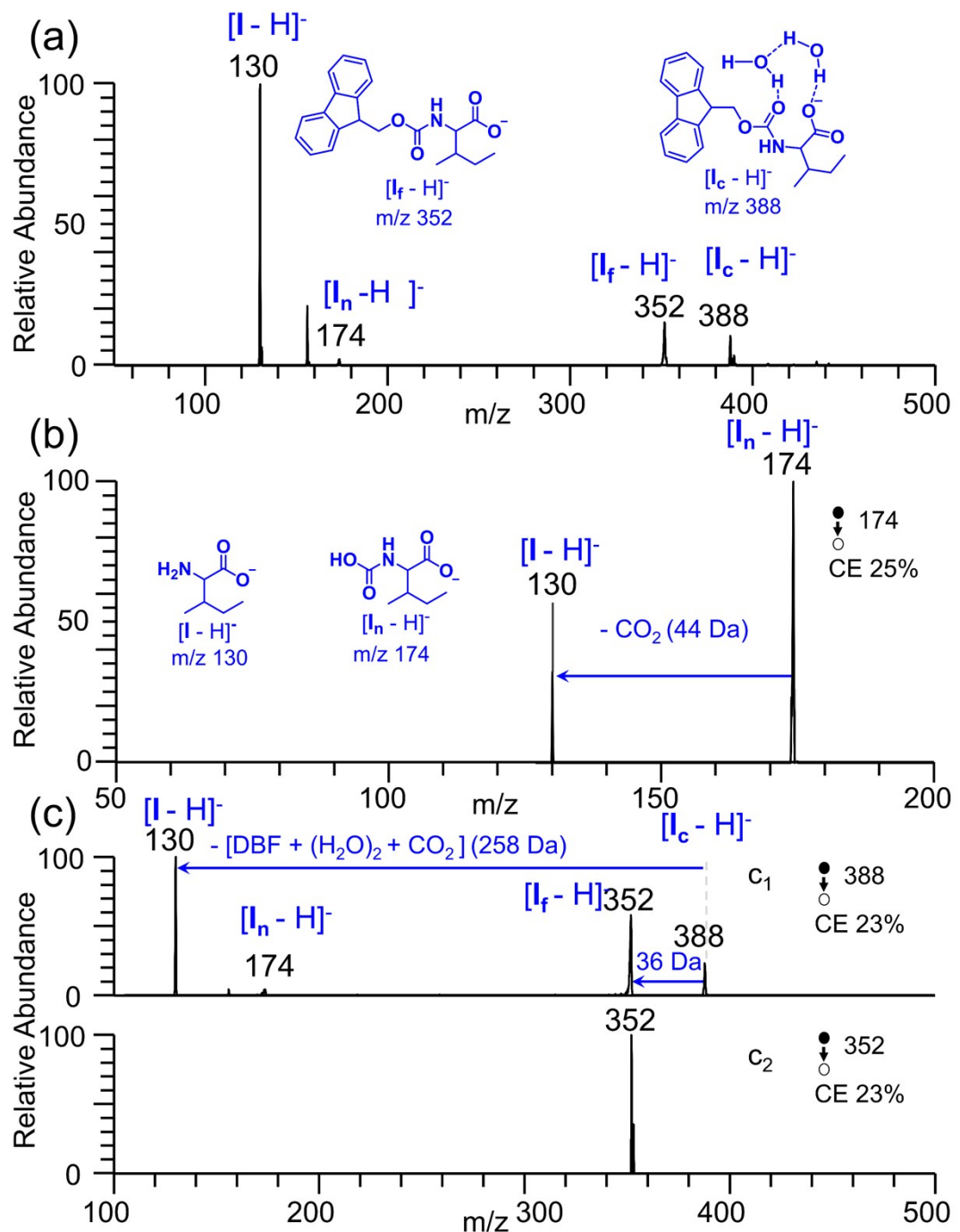


Figure S8. Mass spectrometric analysis of Fmoc elimination reaction in microdroplets of **I_f.** (a) Online mass spectrum of Fmoc deprotection reaction of **I_f** in microdroplets. MS/MS spectra of ions of m/z 174 (b), m/z 388 (c₁), m/z 352 (c₂).

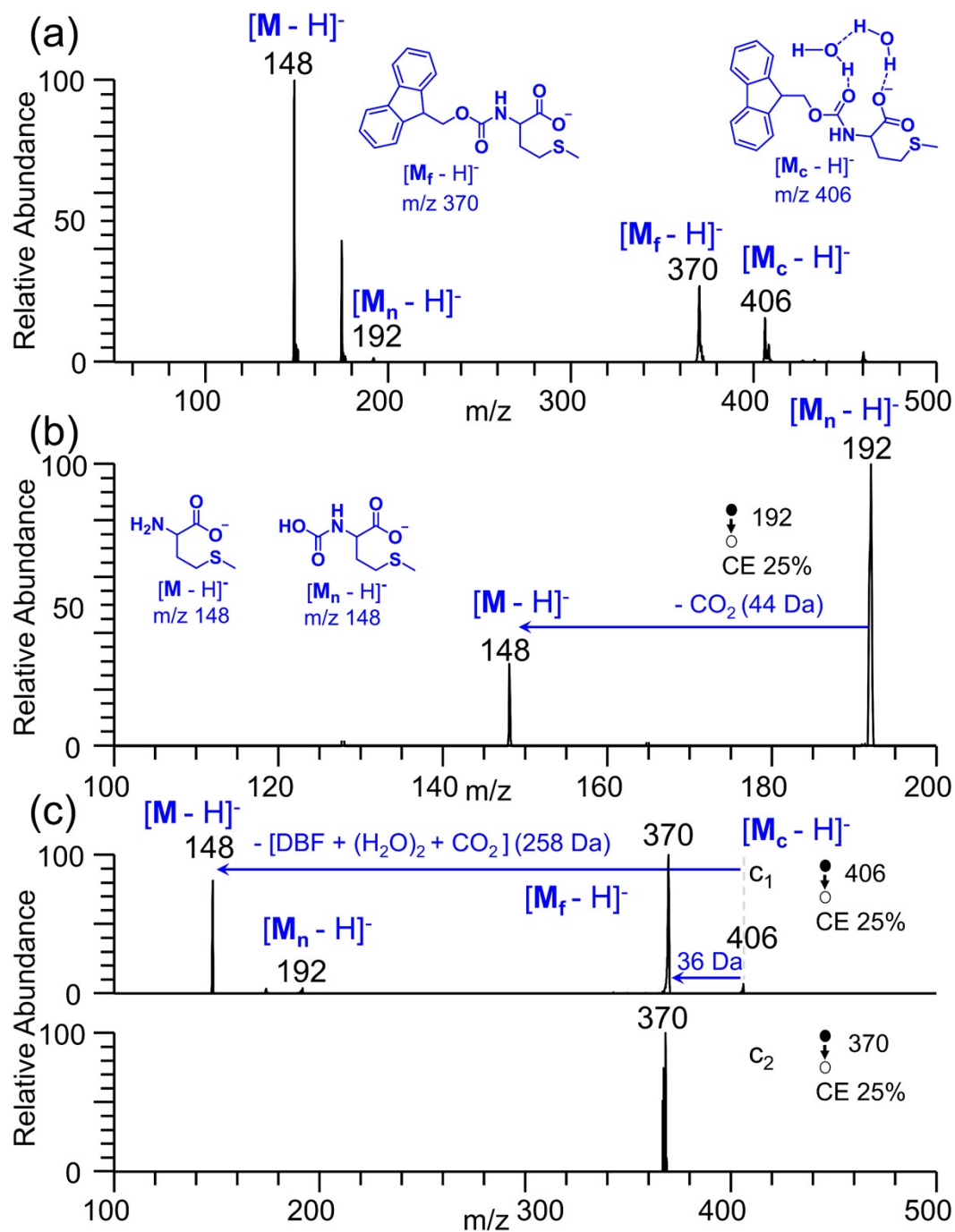


Figure S9. Mass spectrometric analysis of Fmoc elimination reaction in microdroplets of \mathbf{M}_f . (a) Online mass spectrum of Fmoc deprotection reaction of \mathbf{M}_f in microdroplets. MS/MS spectra of ions of m/z 192 (b), m/z 406 (c_1), m/z 370 (c_2).

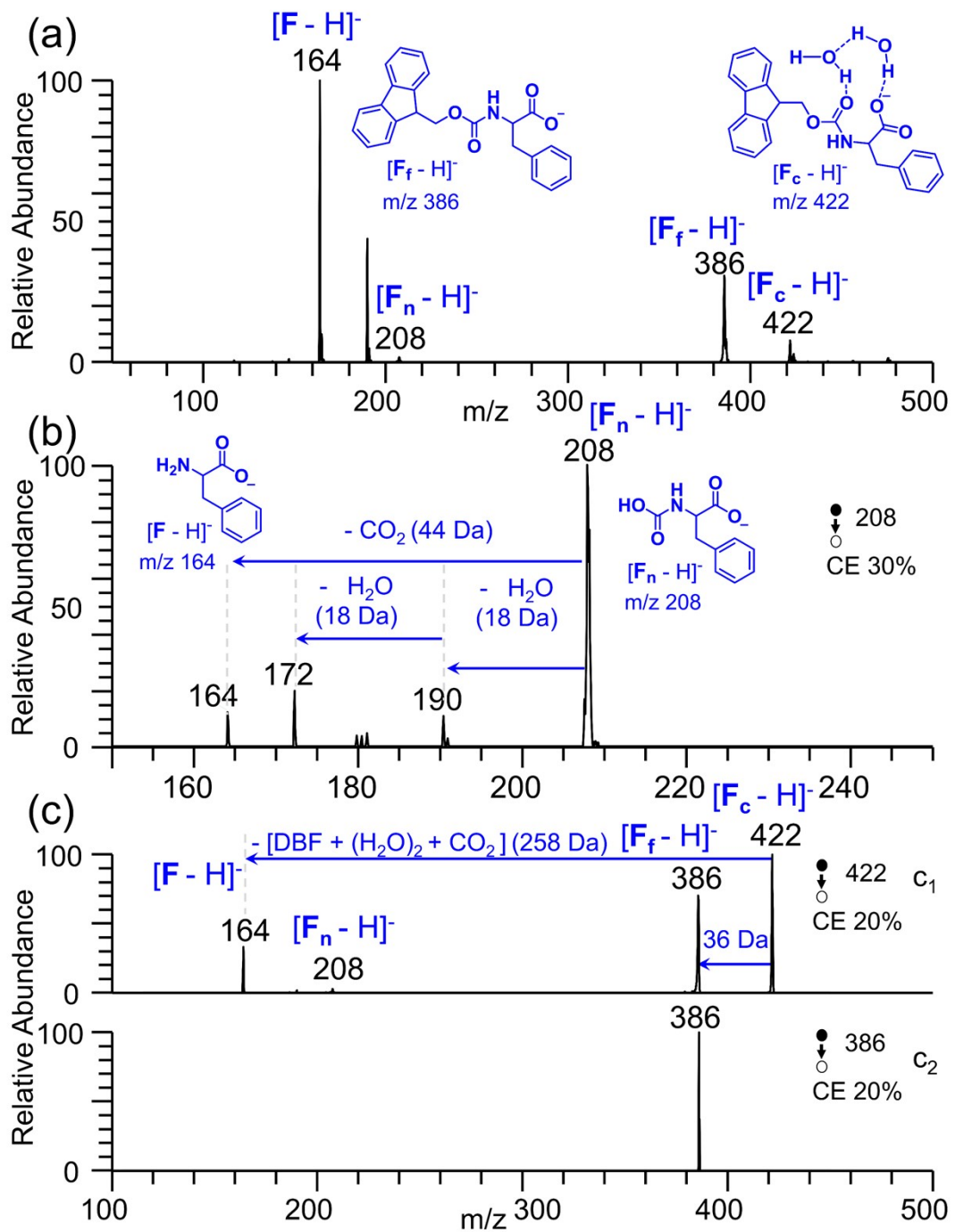


Figure S10. Mass spectrometric analysis of Fmoc elimination reaction in microdroplets of F_f . (a) Online mass spectrum of Fmoc deprotection reaction of F_f in microdroplets. MS/MS spectra of ions of $m/z\ 208$ (b), $m/z\ 422$ (c_1), $m/z\ 386$ (c_2).

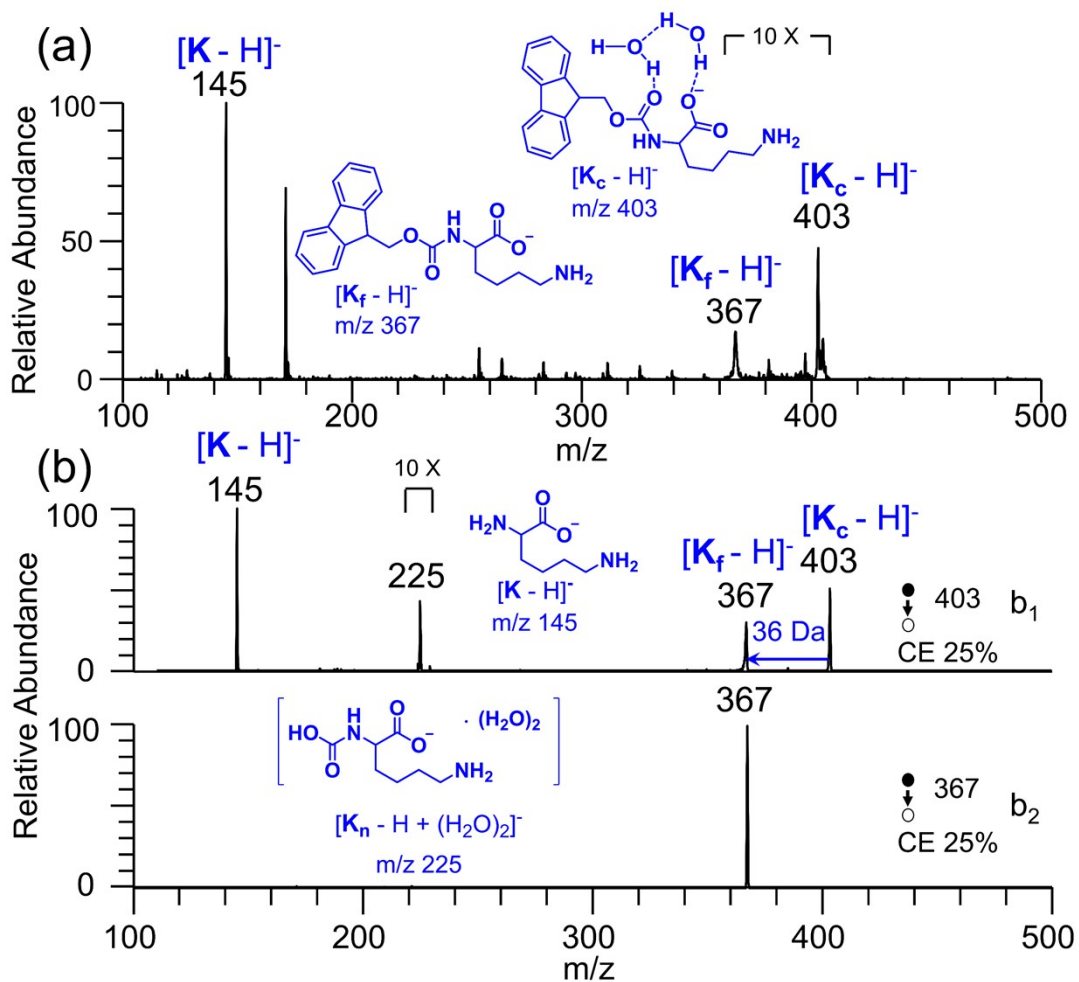


Figure S11. Mass spectrometric analysis of Fmoc deprotection reaction in microdroplets of \mathbf{K}_f . (a) Online mass spectrum of Fmoc deprotection reaction of \mathbf{K}_f in microdroplets. MS/MS spectra of ions of m/z 403 (b₁), m/z 367 (b₂).

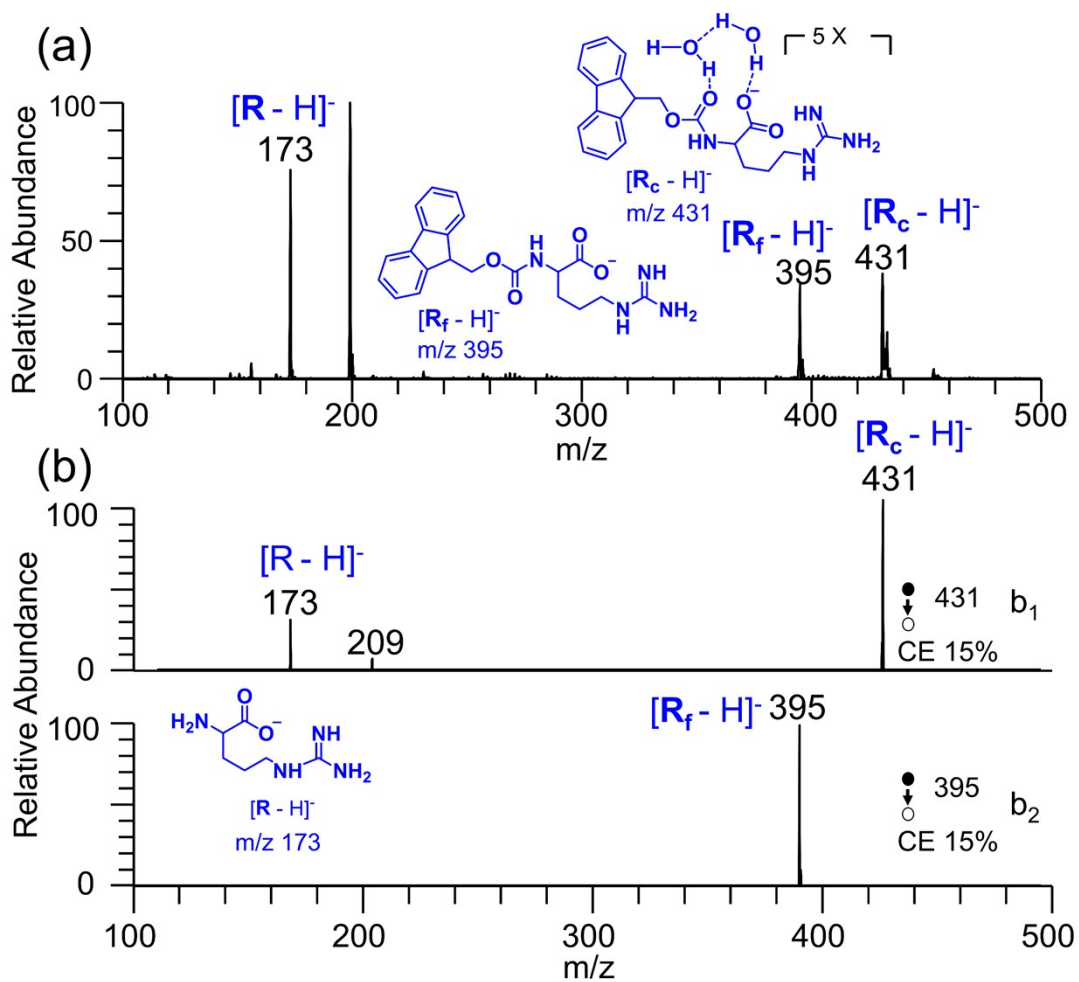


Figure S12. Mass spectrometric analysis of Fmoc elimination reaction in microdroplets of \mathbf{R}_f . (a) Online mass spectrum of Fmoc deprotection reaction of \mathbf{R}_f in microdroplets. MS/MS spectra of ions of m/z 431 (b₁), m/z 395 (b₂).

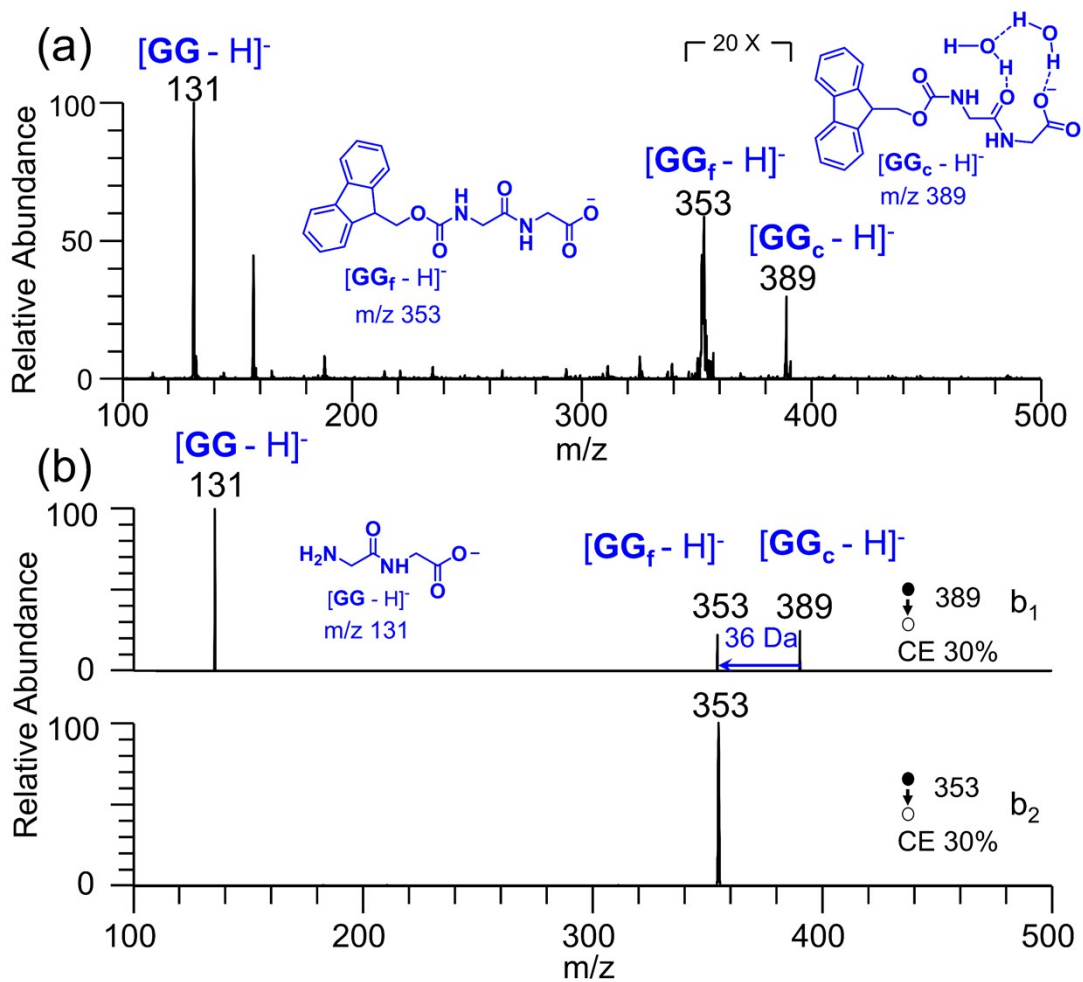


Figure S13. Mass spectrometric analysis of Fmoc elimination reaction in microdroplets of GG_f . (a) Online mass spectrum of Fmoc deprotection reaction of GG_f in microdroplets. MS/MS spectra of ions of $m/z\ 389$ (b_1), $m/z\ 353$ (b_2).

Table S1 Relative proportion of $[X_f - H]^-$ and $[X_c - H]^-$ after microdroplet reaction recorded by mass spectrometer, comparing with base peaks in the mass spectra

Reactant	$[X_f - H]^-$ m/z (%)	$[X_c - H]^-$ m/z (%)
G_f	296 (28)	332 (84)
A_f	310 (10)	346 (48)
P_f	336 (2)	372 (19)
V_f	338 (17)	374 (9)
L_f	352 (14)	388 (11)
I_f	352 (15)	388 (10)
K_f	367 (1.8)	403 (5)
M_f	370 (27)	406 (17)
F_f	386 (31)	422 (8)
R_f	395 (5)	431 (8)
GG_f	353 (3)	389 (1.5)

As for protected lysine (**K_f**), Arginine (**R_f**) and dipeptide (**GG_f**), their relative proportions of $[X_f - H]^-$ are $\leq 5\%$, suggesting that, in microdroplets, $[K_f - H]^-$, $[R_f - H]^-$ and $[GG_f - H]^-$ are more likely to undergo fragmentation and release Fmoc group. As we know, the fragmentation of the protected amino acid highly depends on the release of the lone hydrogen at the ninth carbon of the fluorene ring. It was rationalized that the extra nitrogen atoms in **K_f**, **R_f**, and **GG_f** may act as acceptors for the lone hydrogen at the ninth carbon and promote the release of Fmoc group. The relative low proportion of $[P_f - H]^-$ may owe to the property of secondary amine (proline is a secondary amine and the basicity of a secondary amine commonly higher than that of a primary amine). $[X_c - H]^-$ are ions derived from the combination of $[X_f - H]^-$ with a water dimer via the hydrogen bond. The relative proportions of $[G_c - H]^-$ and $[A_c - H]^-$ are 84% and 48%, respectively. However, the relative proportions of other compounds are much lower than that of $[G_c - H]^-$ and $[A_c - H]^-$, it may due to their large substitutes on the side chain which may hinder the water dimer binding to the

two carboxyl groups of $[X_c - H]$. The relative low proportion of $[GG_c - H]^-$ may due to the intramolecular hydrogen bonding of $[GG_f - H]^-$, which may occupy the binding sites of the water dimer.

Cartesian coordinates (in angstrom), calculated gas-phase Gibbs free energies and gas-phase enthalpies of all intermediates and transition states.

P_f

ΔG_{gas} = -1126.398682 a.u.

ΔH_{gas} = -1126.329051 a.u.

1	C	0.000000337	0.000001058	-0.000000679
2	C	-0.000001228	0.000001104	0.000000370
3	C	0.000002314	-0.000001727	-0.000000674
4	C	-0.000001607	0.000001380	0.000000925
5	C	0.000000044	0.000000203	-0.000000270
6	C	0.000000072	-0.000001638	-0.000000366
7	H	0.000000387	-0.000000672	-0.000000889
8	H	-0.000000360	-0.000000854	-0.000000742
9	H	-0.000001833	0.000000282	-0.000000136
10	H	0.000000373	-0.000000052	-0.000000711
11	C	0.000004667	-0.000001266	-0.000004153
12	H	-0.000004386	0.000001538	0.000000861
13	C	-0.000001925	-0.000000598	0.000000440
14	C	0.000000038	-0.000002415	-0.000001192
15	C	0.000000654	-0.000000263	-0.000000405
16	C	-0.000000054	-0.000000429	-0.000000060
17	C	-0.000000257	-0.000000215	-0.000000862
18	C	0.000000592	-0.000000855	-0.000000468
19	H	-0.000000497	0.000000150	0.000000760
20	H	-0.000000224	0.000000438	0.000000199
21	H	0.000000640	0.000000208	0.000000002
22	H	0.000000747	-0.000000341	-0.000000517
23	C	-0.000004789	-0.000004042	-0.000001937
24	H	-0.000001089	0.000003430	0.000000190
25	H	-0.000000350	-0.000000545	0.000000324
26	O	-0.000003168	-0.000003933	-0.000001671
27	C	0.000006847	0.000016749	0.000001507
28	O	-0.000001960	-0.000003456	0.000002905
29	C	0.000007891	-0.000008735	-0.000004653
30	C	0.000003202	0.000000152	-0.000002131
31	C	-0.000000279	0.000006263	0.000009142
32	H	0.000001370	-0.000000529	-0.000000201
33	C	-0.000006315	-0.000001796	-0.000006710
34	H	0.000000247	-0.000000195	0.000003110
35	H	-0.000001123	-0.000005296	-0.000001901
36	H	-0.000005212	-0.000000090	0.000008083
37	H	0.000002539	-0.000002081	0.000000373

38	H	0.000001425	0.000005633	-0.000007210
39	H	-0.000001411	0.000001168	0.000005334
40	N	0.000002404	0.000005004	-0.000004031
41	C	-0.000003401	0.000007383	-0.000003448
42	O	0.000001348	-0.000001936	0.000006330
43	O	0.000003329	-0.000008183	0.000005164

H₂O

ΔG_{gas} = -76.273322 a.u.

ΔH_{gas} = -76.251236 a.u.

1	H	-0.000022055	-0.000007943	0.000018427
2	H	0.000005915	-0.000029035	0.000002866
3	O	0.000016140	0.000036978	-0.000021293

P_c

ΔG_{gas} = -1278.971124 a.u.

ΔH_{gas} = -1278.888587 a.u.

1	C	0.000000083	0.000001085	-0.000000065
2	C	-0.000000245	0.000000016	-0.000000357
3	C	0.000000179	-0.000001137	-0.000001190
4	C	-0.000004863	0.000001689	0.000002231
5	C	0.000000556	0.000001801	-0.000000864
6	C	0.000000204	0.000000111	-0.000000450
7	H	-0.000000444	0.000001145	-0.000000722
8	H	-0.000001023	0.000000671	-0.000000852
9	H	-0.000000367	0.000000873	-0.000000423
10	H	0.000000002	0.000000742	-0.000000151
11	C	0.000009888	-0.000003738	-0.000011289
12	H	-0.000003600	0.000002785	0.000003251
13	C	-0.000001775	0.000006637	0.000002567
14	C	0.000001996	-0.000005014	-0.000000779
15	C	-0.000002008	0.000001998	0.000000374
16	C	0.000002252	0.000002896	0.000001103
17	C	0.000000059	-0.000002702	0.000000557
18	C	0.000000383	-0.000000491	-0.000001590
19	H	0.000000964	0.000001047	0.000000961
20	H	0.000001221	-0.000000040	0.000000429
21	H	0.000000651	0.000000359	-0.000000116
22	C	0.000000549	0.000001012	0.000000266
23	C	-0.000010246	0.000020634	0.000012479

24	H	0.000002225	-0.000002673	-0.000001746
25	H	0.000001770	-0.000002723	0.000000643
26	O	0.000005369	-0.000022164	-0.000015090
27	C	0.000013523	0.000014839	0.000002695
28	O	-0.000002518	-0.000005438	0.000002298
29	C	0.000011665	-0.000002831	0.000000837
30	C	-0.000001376	-0.000004622	0.000000521
31	C	-0.000005400	0.000002562	-0.000001398
32	H	-0.000000843	-0.000001689	-0.000001189
33	C	0.000002229	0.000002504	0.000001041
34	H	-0.000000650	-0.000000582	0.000000495
35	H	-0.000000631	0.000000624	-0.000000044
36	H	0.000002278	-0.000001395	0.000000931
37	H	0.000001255	-0.000001028	0.000000116
38	H	0.000000423	-0.000001827	0.000000864
39	H	0.000000800	-0.000000992	0.000000796
40	N	-0.000015138	-0.000001559	0.000006662
41	C	-0.000021952	-0.000017144	0.000003226
42	O	0.000009270	0.000023561	-0.000032710
43	O	0.000006484	-0.000000937	0.000002797
44	O	-0.000004719	-0.000000355	-0.000000670
45	H	0.000005729	-0.000011165	-0.000000879
46	H	0.000000499	-0.000000743	0.000001180
47	O	0.000021822	0.000026530	-0.000007121
48	H	-0.000018006	-0.000006150	-0.000002009
49	H	-0.000008522	-0.000016980	0.000032384

TS1 (315.45 icm⁻¹)

$\Delta G_{\text{gas}} = -1126.370974$ a.u.

$\Delta H_{\text{gas}} = -1126.301022$ a.u.

1	C	-0.000000117	-0.000000586	-0.000000886
2	C	-0.000000220	-0.000000331	-0.000000980
3	C	-0.000000259	-0.000000196	-0.000000709
4	C	0.000000047	-0.000000295	-0.000000570
5	C	0.000000002	-0.000000406	-0.000000356
6	C	-0.000000003	-0.000000541	-0.000000555
7	H	-0.000000114	-0.000000694	-0.000001054
8	H	-0.000000298	-0.000000378	-0.000001267
9	H	-0.000000265	-0.000000021	-0.000000857
10	H	0.000000112	-0.000000640	-0.000000438
11	C	-0.000000098	-0.000000716	0.000000041
12	H	0.000000074	0.000001590	-0.000000685

13	C	-0.000000128	-0.000000374	0.000000383
14	C	0.000000233	-0.000000092	0.000000496
15	C	0.000000219	0.000000043	0.000000702
16	C	0.000000213	-0.000000200	0.000000590
17	C	0.000000224	-0.000000413	0.000000270
18	C	0.000000105	-0.000000262	-0.000000014
19	H	0.000000178	0.000000396	0.000000581
20	H	0.000000339	0.000000042	0.000000972
21	H	0.000000404	-0.000000303	0.000000799
22	H	0.000000317	-0.000000514	0.000000220
23	C	0.000000058	0.000000643	0.000000007
24	H	-0.000000230	0.000000502	0.000000042
25	H	-0.000000280	0.000000585	-0.000000510
26	O	0.000000047	-0.000000726	-0.000000471
27	C	-0.000000164	0.000000151	-0.000001517
28	O	0.000001292	-0.000000841	0.000001670
29	C	0.000000684	-0.000000365	0.000003794
30	C	-0.000001168	0.000003061	-0.000003490
31	C	-0.000001465	0.000005445	-0.000001726
32	H	0.000000269	-0.000000720	0.000000382
33	C	-0.000002298	-0.000005166	0.000001459
34	H	0.000001233	0.000001969	0.000000414
35	H	-0.000001287	0.000000763	0.000000271
36	H	0.000000648	0.000000716	0.000000464
37	H	0.000000145	0.000000032	-0.000000437
38	H	0.000000164	-0.000000680	-0.000000407
39	H	0.000000196	-0.000000384	0.000001621
40	N	0.000001563	-0.000001102	-0.000001452
41	C	0.000000182	0.000001028	0.000002010
42	O	-0.000001219	0.000000009	0.000000405
43	O	0.000000665	-0.000000028	0.000000791

TS2 (544.60 cm^{-1})

$\Delta G_{\text{gas}} = -1278.954270$ a.u.

$\Delta H_{\text{gas}} = -1278.876798$ a.u.

1	C	0.000000430	-0.000000380	0.000000446
2	C	-0.000000892	0.000000442	0.000000528
3	C	-0.000001070	-0.000000379	-0.000000864
4	C	0.000000352	0.000005348	-0.000001081
5	C	0.000002235	0.000000345	-0.000000956
6	C	0.000000034	0.000000618	0.000001362
7	H	0.000000148	-0.000000171	0.000000733

8	H	0.000000169	-0.000000174	0.000000360
9	H	0.000000138	0.000000051	0.000000034
10	H	0.000000075	-0.000000188	0.000000741
11	C	0.000010076	0.000044536	-0.000015595
12	H	-0.000050242	-0.000112032	0.000056155
13	C	-0.000004321	0.000001085	-0.000006095
14	C	-0.000013861	-0.000000585	-0.000022055
15	C	0.000000453	-0.000001591	-0.000001587
16	C	-0.000001245	-0.000001480	0.000002149
17	C	-0.000002331	0.000002534	0.000000502
18	C	0.000002539	-0.000001534	0.000003013
19	H	-0.000003835	0.000001140	-0.000008334
20	H	-0.000000092	-0.000000013	-0.000000167
21	H	-0.000000463	-0.000000023	0.000000152
22	H	-0.000000188	-0.000000059	0.000000711
23	C	-0.000004412	0.000012643	0.000001672
24	H	0.000000930	-0.000001160	-0.000007150
25	H	-0.000001797	-0.000002743	0.000001935
26	O	0.000021018	-0.000020333	-0.000006332
27	C	-0.000019200	0.000006923	0.000014665
28	O	0.000008607	0.000007491	-0.000018695
29	C	0.000009118	-0.000005481	-0.000000939
30	C	-0.000003103	-0.000002597	0.000000676
31	C	-0.000003547	0.000001366	-0.000002980
32	H	0.000000579	0.000006645	0.000003936
33	C	-0.000000849	-0.000002423	0.000003816
34	H	0.000000062	-0.000000893	-0.000001549
35	H	-0.000001497	-0.000000740	0.000001619
36	H	0.000005736	0.000002776	0.000002541
37	H	0.000000898	-0.000007971	0.000002031
38	H	-0.000005106	0.000004140	-0.000001515
39	I	0.000003728	0.000000204	-0.000005129
40	N	-0.000014389	0.000011035	0.000008656
41	C	0.000002682	0.000016027	-0.000002620
42	O	-0.000018429	0.000016907	0.000013963
43	O	-0.000001005	-0.000002913	-0.000001474
44	O	0.000299390	-0.000049098	0.000177100
45	H	-0.000431985	0.000231739	-0.000391922
46	H	-0.000002195	-0.000032458	0.000010364
47	O	0.000203859	-0.000100673	0.000189507
48	H	0.000012662	-0.000032989	-0.000005252
49	H	0.000000135	0.000007087	0.000002922

Int1 $\Delta G_{\text{gas}} = -740.604085 \text{ a.u.}$ $\Delta H_{\text{gas}} = -740.545244 \text{ a.u.}$

1	C	-0.000001812	-0.000002820	0.000000406
2	O	0.000001872	0.000001035	0.000000649
3	C	0.000001443	-0.000005758	-0.000002298
4	C	-0.000004741	-0.000000237	-0.000000502
5	C	-0.000003266	-0.000001355	0.000000550
6	H	-0.000001203	0.000002112	0.000000686
7	C	0.000009630	-0.000002070	-0.000002999
8	H	-0.000002902	-0.000001537	0.000001689
9	H	-0.000000681	0.000001380	0.000001339
10	H	0.000000506	0.000000569	-0.000001197
11	H	0.000000219	0.000002501	0.000000012
12	H	0.000000687	0.000000555	0.000000694
13	H	0.000000073	-0.000001090	-0.000000340
14	N	0.000005216	0.000004051	0.000000417
15	C	0.000005321	0.000014676	-0.000004111
16	O	-0.000000529	-0.000013882	0.000014744
17	O	-0.000020477	0.000011137	0.000007616
18	O	-0.000000520	0.000001462	0.000000804
19	H	0.000000020	0.000001068	0.000001455
20	O	-0.000008507	-0.000010556	0.000003307
21	H	0.000000957	0.000001285	-0.000029734
22	H	0.000003369	0.000006092	0.000005924
23	O	-0.000001442	0.000008446	-0.000000350
24	H	0.000014815	-0.000018941	-0.000006953
25	H	0.000001948	0.000001876	0.000008192

P_n $\Delta G_{\text{gas}} = -588.025229 \text{ a.u.}$ $\Delta H_{\text{gas}} = -587.977952 \text{ a.u.}$

1	C	-0.000003344	0.000010896	-0.000001669
2	O	-0.000001407	-0.000000422	0.000003050
3	C	0.000009259	-0.000019258	0.000037412
4	C	-0.000029590	-0.000046854	0.000006458
5	C	-0.000013756	0.000012874	-0.000001186
6	H	-0.000000150	0.000002194	-0.000002639
7	C	0.000029133	-0.000021583	-0.000009564
8	H	-0.000005692	0.000015448	-0.000000178

9	H	-0.000006836	-0.000008184	0.000001782
10	H	-0.000004674	0.000004774	-0.000008536
11	H	0.000001875	-0.000001098	0.000000287
12	H	0.000014011	0.000005555	-0.000007399
13	H	0.000006225	-0.000002315	0.000015572
14	N	0.000027983	0.000033237	-0.000036085
15	C	-0.000046449	0.000003350	0.000018004
16	O	0.000003542	0.000011089	-0.000010521
17	O	0.000013898	0.000004325	-0.000010293
18	O	0.000009402	-0.000002625	0.000006706
19	H	-0.000003431	-0.000001404	-0.000001202

References

- [1] M. J. Frisch, G. W. Trucks, H. B. Schlegel, G. E. Scuseria, M. A. Robb, J. R. Cheeseman, G. Scalmani, V. Barone, G. A. Petersson, H. Nakatsuji, X. Li, M. Caricato, A. V. Marenich, J. Bloino, B. G. Janesko, R. Gomperts, B. Mennucci, H. P. Hratchian, J. V. Ortiz, A. F. Izmaylov, J. L. Sonnenberg, Williams, F. Ding, F. Lipparini, F. Egidi, J. Goings, B. Peng, A. Petrone, T. Henderson, D. Ranasinghe, V. G. Zakrzewski, J. Gao, N. Rega, G. Zheng, W. Liang, M. Hada, M. Ehara, K. Toyota, R. Fukuda, J. Hasegawa, M. Ishida, T. Nakajima, Y. Honda, O. Kitao, H. Nakai, T. Vreven, K. Throssell, J. A. Montgomery Jr., J. E. Peralta, F. Ogliaro, M. J. Bearpark, J. J. Heyd, E. N. Brothers, K. N. Kudin, V. N. Staroverov, T. A. Keith, R. Kobayashi, J. Normand, K. Raghavachari, A. P. Rendell, J. C. Burant, S. S. Iyengar, J. Tomasi, M. Cossi, J. M. Millam, M. Klene, C. Adamo, R. Cammi, J. W. Ochterski, R. L. Martin, K. Morokuma, O. Farkas, J. B. Foresman, D. J. Fox, Gaussian 16 A.03. Wallingford, CT, **2016**.
- [2] S. Grimme, S. Ehrlich and L. Goerigk, *J. Comput. Chem.*, 2011, **32**, 1456-1465.
- [3] J.-D. Chai and M. Head-Gordon, *Phys. Chem. Chem. Phys.*, 2008, **10**, 6615-6620.
- [4] F. Weigend and R. Ahlrichs, *Phys. Chem. Chem. Phys.*, 2005, **7**, 3297-3305.
- [5] K. Fukui, *Acc. Chem. Res.*, 1981, **14**, 363-368.
- [6] Semichem, Inc., GaussView 6.0.16 program: <http://gaussian.com/gaussview6/> (accessed on Nov 25, 2019).